

# Non-collinear magnetoconductance of a quantum dot

Jonas Nyvold Pedersen<sup>1,2</sup>, Jesper Qvist Thomassen<sup>1</sup>, and Karsten Flensberg<sup>1</sup>

<sup>1</sup>*Ørsted Laboratory, Niels Bohr Institute, Universitetsparken 5, 2100 Copenhagen, Denmark.*

<sup>2</sup>*Department of Physics, University of Lund, Box 118, 22100 Lund, Sweden.*

(Dated: December 2, 2024)

We study theoretically the conductance of a quantum dot connected to ferromagnetic leads. The dot level is split due to a non-collinear magnetic field or intrinsic magnetization. The system is studied for non-interacting electrons, where an exact solution is given, and, furthermore, with Coulomb interactions in the weak tunneling limit. For the non-interacting case, we find an anti-resonance when the field is perpendicular to the (parallel) magnetization directions of the leads. The anti-resonance is destroyed by the interaction, giving rise to an interaction induced enhancement of the conductance. When the lead magnetizations are anti-parallel the interaction does not alter the angle dependence significantly. The angular dependence can thus be used to measure the importance of correlations in the transport.

Spin transport through hybrid structures of both semiconductor and metal systems is now a well-established field of research<sup>1</sup>. In recent years, also spin transport through quantum dots formed by nanotubes, molecular systems or nanoparticles has started to attract attention both experimentally<sup>2,3,4,5,6,7,8</sup> and theoretically<sup>9,10,11,12</sup>. One of the motivations for this has been the possibility of using quantum dots with a single spin as qubits, but naturally also a number of fundamental questions arise on how the interplay of spin coherence and interactions influences the transport.

In this paper, we address the conductance of a quantum dot modelled by a single level with spin degree of freedom. The quantum system is connected to ferromagnetic leads, and in addition the spin states of the quantum dot are split due to, e.g., an applied magnetic field. The magnetic field is assumed to be non-collinear to the magnetizations of the leads, and this turns out to give rise to interesting interference effects. Experimentally, one could realize this geometry if the magnetic leads are fabricated as magnetic thin films, where the magnetic field is strongly pinned in the plane parallel to the film, such that a small magnetic field component can be applied to the quantum dot without changing the magnetization direction of the leads. The geometry of the device is illustrated in Fig. 1. We describe the system using a modified Anderson Hamiltonian where the leads are assumed polarized and the magnetic field gives

rise to an energy splitting of the dot level. This gives an effective double-slit geometry with two different paths through the central region. In case of parallel magnetizations of the leads and no Coulomb repulsion on the dot, we find sharp anti-resonances in the conductance for certain angles  $\phi$  which is explained as destructive interference. If the Coulomb repulsion on the dot is increased a cross-over to a simple spin-valve behavior is seen. Changing the angle  $\phi$  in an experimental setup can therefore indicate if interactions on the dot are important or if a single-electron picture is sufficient. On the contrary, in case of anti-parallel magnetizations of the leads no change in the angular dependence is observed when the Coulomb repulsion on the dot is increased.

The model Hamiltonian of the quantum dot coupled to magnetic leads is

$$H = H_{LR} + H_T + H_D, \quad (1)$$

where

$$H_{LR} = \sum_{\alpha=L,R,k\sigma} \xi_{\alpha,k\sigma} c_{\alpha,k\sigma}^\dagger c_{\alpha,k\sigma}, \quad (2)$$

where  $\alpha$  denotes the left or right electrode and where we have assumed that the polarizations of the electrodes are parallel or anti-parallel. The magnetization of the quantum dot is not necessary parallel to those of the leads and in the spin basis of the leads, the dot Hamiltonian is

$$H_D = \sum_{\sigma} \xi_0 d_{\sigma}^\dagger d_{\sigma} + U n_{\uparrow} n_{\downarrow} + \sum_{\sigma\sigma'} \mathbf{B} \cdot \boldsymbol{\sigma}_{\sigma\sigma'} d_{\sigma}^\dagger d_{\sigma'}, \quad (3)$$

where  $\xi_0$  is the orbital quantum dot energy,  $B$  represents the magnetic field splitting, and  $U$  is the Coulomb energy for double occupancy. In a diagonal basis, the dot Hamiltonian is

$$H_D = \sum_{\sigma} (\xi_0 + \sigma B) \tilde{d}_{\sigma}^\dagger \tilde{d}_{\sigma} + U \tilde{n}_{\uparrow} \tilde{n}_{\downarrow}, \quad (4)$$

where the  $d$  and  $\tilde{d}$  operators are related by the unitary

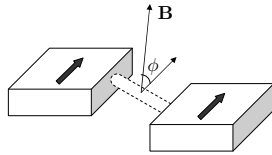


FIG. 1: Schematic drawing of the quantum dot system, connected to two ferromagnetic leads. In addition, there is an applied magnetic which spin polarizes the quantum dot in a direction non-collinear to the magnetization of the leads. In this paper, we focus on how the conductance depends on the angle  $\phi$ , and the interplay between interactions and spin interference.

rotation

$$d_\sigma = \sum_{\sigma'} R_{\sigma\sigma'} \tilde{d}_{\sigma'}, \quad \mathbf{R} = \begin{pmatrix} \cos(\phi/2) & \sin(\phi/2) \\ -\sin(\phi/2) & \cos(\phi/2) \end{pmatrix}. \quad (5)$$

Finally, the tunneling Hamiltonian is

$$H_T = \sum_{\alpha=L,R,k\sigma\sigma'} \left( t_{\alpha,k\sigma} R_{\sigma\sigma'} c_{\alpha,k\sigma}^\dagger \tilde{d}_{\sigma'} + \text{h.c.} \right). \quad (6)$$

Here we allow for the tunneling matrix element to be spin dependent, because the states in the leads depend on spin direction. However, spin flip processes during the tunneling are assumed small and hence not included.

*Resonant tunneling for the non-interacting case* – We start by discussing the current through the system in absence of interactions, i.e.  $U = 0$ . This is relevant for a system not in the Coulomb blockade or a resonant tunneling junction system. The conductance follows from the Landauer formula as

$$G = \frac{e^2}{h} \int d\epsilon T(\epsilon) \left( -\frac{\partial n_F(\epsilon)}{\partial \epsilon} \right), \quad (7)$$

where  $T(\epsilon)$  is the total transmission coefficient for both spin directions, and  $n_F$  is the Fermi-Dirac distribution function. In terms of the retarded and advanced Green's function the transmission coefficient is<sup>13</sup>

$$T(\epsilon) = \text{Tr} [\mathbf{G}^a(\epsilon) \Gamma^R(\epsilon) \mathbf{G}^r(\epsilon) \Gamma^L(\epsilon)], \quad (8)$$

with (using the spin basis where  $H_D$  is diagonal)

$$\mathbf{G}^{r,a}(\epsilon) = (\mathbf{G}_0^{-1} - \Sigma_L^{r,a}(\epsilon) - \Sigma_R^{r,a}(\epsilon))^{-1}, \quad (9a)$$

$$[\mathbf{G}_0(\epsilon)]_{\sigma\sigma'} = \delta_{\sigma,\sigma'} (\epsilon - \xi_0 - \sigma B)^{-1}, \quad (9b)$$

$$[\Sigma_\alpha^{r,a}(\epsilon)]_{\sigma\sigma'} = \sum_{k\sigma''} (R^\dagger)_{\sigma\sigma''} |t_{\alpha,k\sigma''}|^2 g_{\alpha,k\sigma''}^{r,a}(\epsilon) R_{\sigma''\sigma'}, \quad (9c)$$

where  $g_{\alpha,k\sigma}^{r,a}(\epsilon) = (\epsilon - \xi_{\alpha,k\sigma} \pm i0^+)^{-1}$  and  $\Gamma_\alpha = -i[\Sigma_\alpha^r - \Sigma_\alpha^a]$ . In order to simplify the analysis, we assume that parts corresponding to the real parts of  $g^{r,a}$  give constant shift of  $\xi_0$  and hence can be incorporated in  $\mathbf{G}_0$ , and, furthermore, that the tunnel width functions  $\Gamma_{L,R}$  are constant in energy. With these assumptions

$$\Gamma_{L,R}(\epsilon) \frac{\Gamma_{L,R}^0}{2} \begin{pmatrix} 1 + P_{L,R} \cos \phi & P_{L,R} \sin \phi \\ P_{L,R} \sin \phi & 1 - P_{L,R} \cos \phi \end{pmatrix}, \quad (10)$$

where

$$\Gamma_\alpha^0 = 2\pi \sum_{k\sigma} |t_{\alpha,k\sigma}|^2 \delta(\epsilon - \xi_{\alpha,k\sigma}) = \sum_\sigma \Gamma_{\alpha,\sigma}^0, \quad (11)$$

and  $P_\alpha$  denotes the polarization of the tunneling from lead  $\alpha$  defined through  $\Gamma_{\alpha,\sigma}^0 = \frac{1}{2}(1 + \sigma P_\alpha) \Gamma_\alpha^0$ . Finally, we have

$$\mathbf{G}^{r,a}(\epsilon) = ([\mathbf{G}_0^{r,a}(\epsilon)]^{-1} \pm i(\Gamma_L + \Gamma_R)/2)^{-1}. \quad (12)$$

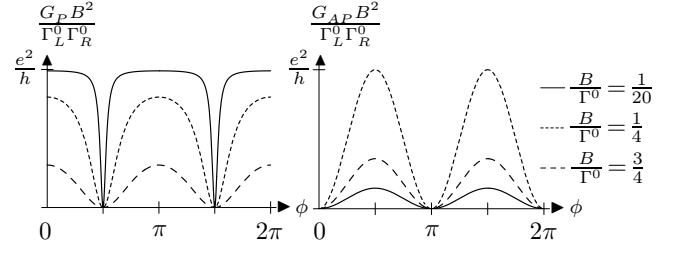


FIG. 2: The conductance for the non-interacting case in both the parallel (left panel) and the anti-parallel (right panel) cases for different values of the magnetic strength and at the symmetric point  $\xi_0 = 0$ . For the parallel case, destructive interference leads to an anti-resonance for  $\phi = \pi/2$ . The anti-resonance sharpens as  $B/\Gamma^0$  decreases. The conductance is maximal when the applied field is parallel to magnetizations in the leads ( $\phi = 0$  or  $\pi$ ). In contrast, for the anti-parallel case the current is maximal for  $\phi = \pi/2$  and vanishes at  $\phi = 0$  and  $\pi$  because of the spin-valve effect.

With these formulae it is straightforward to find the transmission coefficient.

In the following we study the current using the simplifying case of fully polarized leads, i.e. half-metallic contacts. For the parallel configuration,  $P_L = P_R = 1$ , we obtain for the transmission function

$$T_P(\epsilon) = \frac{\Gamma_L^0 \Gamma_R^0}{B^2} \frac{[x - \cos \phi]^2}{(1 - x^2)^2 + y^2 (x - \cos \phi)^2}, \quad (13)$$

where

$$x = \frac{\epsilon - \xi_0}{B}, \quad y = \frac{\Gamma_L^0 + \Gamma_R^0}{2B} = \frac{\Gamma^0}{2B}. \quad (14)$$

Let us look at the resonance condition  $x = 0$ , where the incoming energy lies symmetrically between the spin split levels:

$$T_P(\xi_0) = \frac{\Gamma_L^0 \Gamma_R^0}{B^2} \frac{\cos^2 \phi}{1 + y^2 \cos^2 \phi}. \quad (15)$$

This yields a sharp anti-resonance when the dot magnetization is perpendicular to the magnetization direction of the leads. The anti-resonance occurs due to a destructive interference between the transmissions through the two spin split levels, as explained in detail below. It is interesting to note that the zero transmission at  $\phi = \pi/2$  is not broadened by higher order tunneling events, as one might have expected. Moreover, for the non-symmetric situation  $x \neq 0$ , the anti-resonance remains, but is shifted away from  $\phi = \pi/2$  to the point where  $x = \cos \phi$ , which follows from Eq. (13). The anti-resonance found here is in fact similar to an effect exploited in single atom transmission through optical lattices<sup>14</sup>.

Next, we look at the antiparallel situation. Therefore we set  $P_L = -P_R = 1$  and find

$$T_{AP}(\epsilon) = \frac{4\Gamma_L^0 \Gamma_R^0 \sin^2 \phi}{B^2 D}, \quad (16)$$

where

$$D = 4(1 - x^2)^2 + 2y_L y_R + y_L^2 y_R^2 / 4 + (y_R^2 + y_L^2)x^2 + 2(y_L^2 - y_R^2)x \cos \phi + (y_L - y_R)^2 \cos^2 \phi, \quad (17)$$

with  $y_\alpha = \Gamma_\alpha^0 / B$ . Note that for the symmetric coupling  $\Gamma_L^0 = \Gamma_R^0$ , the only angle dependence is the  $\sin^2 \phi$  factor in the numerator. In Fig. 2 we show examples of angle dependence of the conductance for both the parallel and antiparallel cases.

*Cotunneling current for the interacting case* – In the presence of interactions the interesting interference effect discussed above can be significantly changed. Naturally, this is in general a difficult problem to tackle. Here we look at the case where the position of the levels is far from resonance, and a second order perturbation calculation suffices. This is the “cotunneling” regime, where an electron is transferred through the system in a two-electron process. We calculate the current using a scattering formalism and the transition rate per unit time between an initial state  $i$  (with energy  $E_i$ ) and a final state  $f$  (with energy  $E_f$ ) is calculated as

$$\Gamma_{fi} = \frac{2\pi}{\hbar} |\langle f | T | i \rangle|^2 \delta(E_f - E_i), \quad (18)$$

where the transition operator  $\hat{T}$  is

$$\hat{T} = H_T + H_T \frac{1}{E_i - H_0 + i\eta} \hat{T} \quad (19)$$

and  $H_0 = H_{LR} + H_D$ . Subtracting all processes which bring an electron from the left to the right lead,  $\Gamma_{RL}$ , with the opposite process gives the current

$$J = e(\Gamma_{RL} - \Gamma_{LR}). \quad (20)$$

The transition rates will only be calculated to lowest non-vanishing order in the coupling. Thus, in the initial state the leads can be considered as two non-interacting electron gasses (here assumed fully spin-polarized) with different chemical potentials. The probability to find the lead  $\alpha$  in a state  $\nu_\alpha$  is denoted  $W_{\nu_\alpha}$ . Because the leads are non-interacting  $W_{\nu_\alpha}$  satisfies

$$\sum_{\nu_\alpha} W_{\nu_\alpha} \langle \nu_\alpha | c_{\alpha,k\sigma}^\dagger c_{\alpha,k\sigma} | \nu_\alpha \rangle = n_F(\varepsilon_{\alpha,k\sigma} - \mu_\alpha). \quad (21)$$

Moreover, the dot is assumed to be in a state where the level with the lower energy  $\varepsilon_\uparrow = \xi_0 - B$  is always occupied and the other energy level always empty, i.e.  $|\mu_\alpha - \varepsilon_\sigma| \gg k_B T, \Gamma^0$ , where  $\Gamma^0 = \Gamma_L^0 + \Gamma_R^0$ . With these simplifications the initial states can be written as  $|i\rangle = |\nu_L, \nu_R, \uparrow\rangle$ , with energy  $E_i = E_{\nu_L} + E_{\nu_R} + \varepsilon_\uparrow$  and probability  $W_{\nu_L} W_{\nu_R}$ .

First, we outline the derivation for  $\Gamma_{RL}$  in the parallel configuration. In the fully polarized case, the leads contain only electrons with one kind of spin, say spin-up, and the final states are  $|f_{kk'}\rangle = c_{R,k\uparrow}^\dagger c_{L,k'\uparrow} |i\rangle$ , meaning that an electron is moved from the left to the right lead in

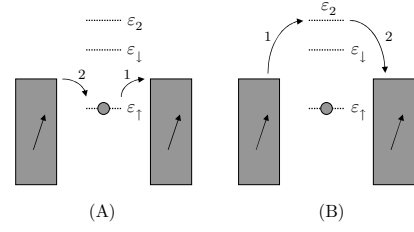


FIG. 3: The two possible second order processes contributing to the tunneling amplitude, here shown for the parallel configuration. Because of interactions, the path to the right is suppressed when the lower energy spin-state is occupied by one electron. Hence the interactions tend to destroy the interference effects seen in Fig. 2, valid for  $U = 0$ , and instead one gets the angular dependence shown in Fig. 4.

the process. Inserting the expressions for the final states and the tunneling Hamiltonian in Eqs. (18) and (19), we see that the first non-vanishing term is second order in the coupling  $H_T$ . Moreover, only two processes gives a contribution: A) first the electron on the dot jumps to the right lead and later an electron from the left lead refills the dot or B) a right lead electron enters the dot, creating a double occupied state, and later leaves the dot to the right. The two processes are sketched in Fig. 3. The scattering rate  $\Gamma_{RL}^{(2)}$  can now be written as

$$\Gamma_{RL}^{(2)} = \frac{2\pi}{\hbar} \sum_{kk'\nu_L\nu_R} W_{\nu_L} W_{\nu_R} |M_A + M_B|^2 \delta(\varepsilon_{R,k\uparrow} - \varepsilon_{L,k'\uparrow}), \quad (22)$$

where

$$M_A = \sum_{k_1 k_2} t_{L,k_2\uparrow}^* t_{R,k_1\uparrow} |R_{\uparrow,\uparrow}|^2 \quad (23)$$

$$\times \langle f_{kk'} | \tilde{d}_\uparrow^\dagger c_{L,k_2\uparrow} \frac{1}{E_i - H_0} c_{R,k_1\uparrow}^\dagger \tilde{d}_\uparrow | i \rangle,$$

$$M_B = \sum_{k_1 k_2} t_{L,k_2\uparrow}^* t_{R,k_1\uparrow} |R_{\downarrow,\uparrow}|^2 \quad (24)$$

$$\times \langle f_{kk'} | c_{R,k_1\uparrow}^\dagger \tilde{d}_\downarrow \frac{1}{E_i - H_0} \tilde{d}_\downarrow^\dagger c_{L,k_2\uparrow} | i \rangle.$$

The matrix elements  $M_A$  and  $M_B$  are easily calculated, and after inserting the coupling constants in Eq. (11) and assuming them to be independent of energy, we arrive at

$$\Gamma_{RL}^{(2)} = \frac{\Gamma_L^0 \Gamma_R^0}{2\pi} \int d\epsilon \left[ \frac{|R_{\uparrow,\uparrow}|^2}{\varepsilon_\uparrow - \epsilon} - \frac{|R_{\downarrow,\uparrow}|^2}{\epsilon - \varepsilon_\downarrow - U} \right]^2 \times n_F(\epsilon - \mu_L) [1 - n_F(\epsilon - \mu_R)]. \quad (25)$$

For  $\Gamma_{LR}^{(2)}$  exactly the same calculations are carried out and we finally obtain for the current

$$J_P^{(2)} = \frac{e}{\hbar} \frac{\Gamma_L^0 \Gamma_R^0}{2\pi} \int d\epsilon \left[ \frac{|R_{\uparrow,\uparrow}|^2}{\varepsilon_\uparrow - \epsilon} - \frac{|R_{\downarrow,\uparrow}|^2}{\epsilon - \varepsilon_\downarrow - U} \right]^2 \times [n_F(\epsilon - \mu_L) - n_F(\epsilon - \mu_R)]. \quad (26)$$

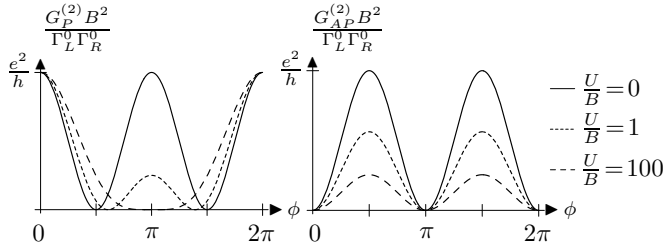


FIG. 4: The conductance for the *interacting* case in both the parallel (left panel) and the anti-parallel (right panel) cases for different values of the Coulomb interaction and for the symmetric point  $\xi_0 = 0$ . For the parallel case, we see how the anti-resonance at  $\phi = \pi/2$  is destroyed by interactions, due to the blocking of one of the paths in Fig. 3. For large  $U$  one instead has a cross-over to a spin-valve effect at  $\phi = \pi$ , where the dot is occupied by an electron with spin opposite to the lead electrons. The angle dependence thus dramatically depends on the interaction. This is not so for the anti-parallel case shown in the right panel, where merely an overall suppressing is seen.

At small bias voltage, we use that  $|\varepsilon| \ll |\varepsilon_\uparrow|, |\varepsilon_\downarrow + U|$  and when inserting the form of  $\mathbf{R}$  from Eq. (5), we obtain

$$J_P^{(2)} = e^2 V \frac{\Gamma_L^0 \Gamma_R^0}{h} \left[ \frac{\cos^2(\phi/2)}{\xi_0 - B} + \frac{\sin^2(\phi/2)}{\xi_0 + B + U} \right]^2, \quad (27)$$

where  $\mu_L - \mu_R = eV$ . The second order (or “cotunneling”) result in Eq. (27) is valid far from resonance, i.e. when the applied  $B$ -field is larger than the bias, temperature and tunneling broadening. The leads have been assumed fully polarized. Note that the two terms in the square brackets are the amplitudes for the two tunneling processes shown in Fig. 3. Of course, a similar calculations can be performed for the antiparallel configuration, and with the same constraints the result is

$$J_{AP}^{(2)} = e^2 V \frac{\Gamma_L^0 \Gamma_R^0}{4h} \left[ \frac{1}{\xi_0 - B} - \frac{1}{\xi_0 + B + U} \right]^2 \sin^2 \phi, \quad (28)$$

which agrees with Eq. (16) in the limits  $U = 0$  and  $\Gamma_{L,R}^0$  small.

The cotunneling results are plotted in Fig. 4 for different values of the Coulomb repulsion  $U$ . It is easily

verified that to second order in  $\Gamma$  and  $U = 0$  the cotunneling results (27) and (28) and the exact results for  $U = 0$  derived above coincide.

*Discussion and summary* – For the non-interacting case, we have explicitly considered the linear response regime at low temperatures. For the parallel configuration, we saw that the angular dependence could be understood in terms of an interference effect occurring due to the spin-splitting of the dot. For  $\phi = 0$  the spin bases of the dot and the leads are identical, and the electrons can only pass through the dot via the spin- $\uparrow$  level. For a non-collinear magnetic field the dot spin eigenstates are superpositions of the lead spin states, which gives two possible paths through the dot. This lead to destructive interference at  $\phi = \pi/2$ , and the resonance sharpened as the tunneling coupling increased. This result was in agreement with the cotunneling result in Eq. (27) setting  $U = 0$ . Interestingly, the destructive interference is destroyed by interactions, giving rise to an interaction induced enhancement of the conductance. Thus the conductance goes from being proportional to  $\cos^2 \phi$  in the non-interacting case to being proportional to  $\cos^4(\phi/2)$  for the strongly interacting case. However, if the leads are not fully polarized the angular dependence persists, but is gradually washed out for decreasing polarization.

For the antiparallel geometry the situation is very different. In the non-interacting case (and symmetric coupling) the conductance is proportional to  $\sin^2 \phi$  for all values of  $\Gamma^0/B$ . This is simply understood as a spin-valve effect, giving zero conductance at  $\phi = 0$  and  $\phi = \pi$ , whereas for non-collinear  $B$ -field the spin can flip when it passes the dot. Furthermore, in this case there is a constructive interference at  $\phi = \pi/2$ . Now, with interactions on the dot one spin channel becomes partially blocked, but the angular dependence remains the same even in the limit of large  $U$ . This is in stark contrast to the cross-over observed for the parallel configuration.

We have thus focused on two cases: 1) strong tunneling and no interaction, and 2) weak tunneling with interaction. The cross-over between these two regime is an interesting and challenging issue, because a formalism that captures both coherence and correlations on equal footing is needed.

<sup>1</sup> I. Zutic, J. Fabian, and S. Das Sarma, Rev. Mod. Phys. **76**, 323 (2004).

<sup>2</sup> K. Tsukagoshi, B. W. Alphenaar, and H. Ago, Nature **401**, 572 (1999).

<sup>3</sup> D. Orgassa, G. J. Mankey, and H. Fujiwara, Nanotechnology **12**, 281 (2001).

<sup>4</sup> X. Hoffer, C. Klinke, J.-M. Bonard, L. Gravier, and J.-E. Wegrowe, cond-mat/0303314.

<sup>5</sup> B. Zhao, I. Mönch, T. Mühl, H. Vinzelberg, and C. M. Schneider, J. Appl. Phys. **91**, 7026 (2002). B. Zhao, I.

Mönch, H. Vinzelberg, T. Mühl, and C. M. Schneider, Appl. Phys. Lett. **80**, 3144 (2002).

<sup>6</sup> J.-R. Kim, H. M. So, J.-J. Kim, and J. Kim, Phys. Rev. B **66**, 233401 (2002).

<sup>7</sup> J. R. Petta, S. R. Slater, and D. C. Ralph, Phys. Rev. Lett. **93**, 136601 (2004).

<sup>8</sup> A. Jensen, J. R. Hauptmann, J. Nygård, and P. E. Lindelof, unpublished.

<sup>9</sup> J. König and J. Martinek, Phys. Rev. Lett. **90**, 166602 (2003).

- <sup>10</sup> W. Rudzinski and J. Barnas, Phys. Rev. B **64**, 085318 (2001).
- <sup>11</sup> J. Martinek et al., Phys. Rev. Lett. **91**, 127203 (2003).
- <sup>12</sup> J. Martinek et al., Phys. Rev. Lett. **91**, 247202 (2003).
- <sup>13</sup> Y. Meir and N.S. Wingreen, Phys. Rev. Lett. **68**, 2512 (1998)
- <sup>14</sup> A. Micheli et al., quant-ph/0406602.